Poincare Journal of Mathematical Physics and Applications
Vol. 1, No. 2 (2026), 97-115
©Poincare Publishers
DOI: 10.46753/pjmpa.2026.v01i02.002
Online Published on 27.11.2026

Modified Adomian Decomposition Methods for Stiff Problems with Stability Analysis and Implicit Runge–Kutta Comparison

Vineet Jassal[1,†] and Dr. Raksha Sharma[2]

[1]Department of Mathematics, Kirori Mal College, University of Delhi, India.
vineetjassal35@gmail.com
[2]Department of Physics, Kirori Mal College, University of Delhi, India.
rakshakmc@kmc.du.ac.in

Submitted: 07.07.2026 | Revised: 01.10.2026 | Accepted: 28.10.2026

Abstract. Stiff initial value problems (IVPs) in chemical kinetics, pharmacokinetics and control theory require numerical methods with large stability regions in the left half-plane. The classical Adomian Decomposition Method (ADM) gives convergent series on short intervals, but truncated ADM behaves like an explicit method and loses stability for stiff systems. This paper studies three strategies: classical truncated ADM, *Multistage ADM* (MADM), which restarts the decomposition on subintervals, and the *Laplace–Adomian Decomposition Method* (LADM), which absorbs a specified linear part through the Laplace transform. For the Dahlquist test equation $y' = \lambda y$, we derive the ADM and MADM stability functions in detail and compare them with the implicit midpoint, trapezoidal and two-stage Radau IIA methods. We prove a convergence theorem for MADM under smoothness and Lipschitz hypotheses and show that the N-term ADM stability function is the degree-$(N-1)$ Taylor polynomial of e^z. Three stiff test problems—a scalar decay, a 2×2 linear stiff system and the nonlinear Van der Pol oscillator—are solved. Exact or tightly controlled reference solutions, uniform error definitions, matched step sizes, work counts and CPU timings are reported to make the comparison reproducible.

Keywords: Adomian decomposition method; multistage ADM; Laplace–Adomian method; stiff problems; stability regions; implicit Runge–Kutta; Van der Pol oscillator
MSC (2020): 65L05, 65L20, 34A34
Communicated by: Shiv k. Kaushik
[†]**Corresponding author**

1. Introduction

The Adomian Decomposition Method (ADM), introduced by George Adomian in the 1980s [3], provides series solutions to linear and nonlinear differential equations without requiring linearisation, perturbation or discretisation [2, 8]. In its classical form, the solution $y(t)$ is expressed as $y(t) = \sum_{n=0}^{\infty} y_n(t)$, and the nonlinear terms are expanded via Adomian polynomials A_n. The method has been successfully applied to a wide variety of ordinary and partial differential equations [21, 12, 4]. Recent work has also examined convergence properties and related decomposition frameworks in broader settings, including PDEs, integral equations, and fractional boundary value problems [19, 16, 10].

However, classical ADM has well-known limitations when applied to *stiff problems* [18, 15]. A system of ODEs is said to be stiff if its eigenvalues λ_i satisfy $|\mathrm{Re}(\lambda_i)| \gg 1$ for at least one eigenvalue, making the ratio $\max|\lambda_i|/\min|\lambda_i|$ large [11]. When truncated to N terms, the classical ADM stability function is the degree-$(N-1)$ Taylor polynomial of e^z and therefore has a bounded stability region.

To address these difficulties, several modifications have been proposed:

- **Multistage ADM (MADM):** The global interval is partitioned into subintervals, and ADM is applied locally on each subinterval, restarting with the endpoint value from the previous subinterval [9, 15, 6]. This reduces the local stability parameter $|z| = |\lambda h|$.
- **Laplace–Adomian Decomposition Method (LADM):** The Laplace transform is applied first to remove the highest-order linear operator and convert it into an algebraic divisor; ADM is then applied in the Laplace domain, and inverse transforms recover the time-domain solution [13, 22].
- **Source-splitting ADM variants:** The source or operator is divided into carefully chosen components to accelerate convergence [20, 14]. We use no abbreviation for this separate family, reserving MADM exclusively for Multistage ADM.

Implicit Runge–Kutta (IRK) methods—such as the implicit midpoint rule, the trapezoidal rule and the Radau IIA family—are the gold standard for stiff problems because they can be made A-stable or L-stable [11, 7]. A systematic comparison of ADM stability regions with those of IRK methods is largely missing from the literature, and the present work aims to fill this gap.

The paper is organised as follows. Section 2 recalls the classical ADM and defines Adomian polynomials. Section 3 introduces the multistage ADM (MADM) and the Laplace–Adomian method (LADM). Section 4 derives the stability functions and regions for truncated ADM and MADM and compares them analytically with implicit Runge–Kutta methods. Section 5 contains convergence and stability theorems. Section 6 presents three stiff test problems with exact solutions, numerical results and error tables. Section 7 concludes.

2. Classical Adomian Decomposition Method

This section summarises the classical ADM framework for initial value problems, including the series representation, Adomian polynomials and the recursive construction of components. The formulation is presented for a general nonlinear operator split and then specialised to

linear problems to highlight how the method reduces to successive integrations. These details set the notation and baseline for later modifications.

2.1. **General formulation.** Consider the general initial value problem

$$\frac{dy}{dt} = f(t, y), \qquad y(0) = y_0, \tag{2.1}$$

where f may contain linear and nonlinear terms. We split the right-hand side as

$$f(t, y) = \mathcal{A}y + \mathcal{N}(y) + g(t),$$

where $\mathcal{A}$ is a linear operator, $\mathcal{N}$ is a nonlinear operator and g is a source term. The time-integration operator is

$$J_t(\varphi) = \int_0^t \varphi(s)\, ds.$$

Applying J_t to (2.1) gives the equivalent Volterra integral equation

$$y(t) = y_0 + J_t\big[\mathcal{A}y + \mathcal{N}(y) + g(t)\big]. \tag{2.2}$$

The ADM assumes a series solution

$$y(t) = \sum_{n=0}^{\infty} y_n(t), \tag{2.3}$$

and decomposes the nonlinear term $\mathcal{N}(y)$ as

$$\mathcal{N}(y) = \sum_{n=0}^{\infty} A_n(y_0, y_1, \ldots, y_n), \tag{2.4}$$

where A_n are the *Adomian polynomials*. Conceptually, the decomposition (2.4) plays the role of a nonlinear analogue of the Taylor expansion: each A_n collects terms of "degree" n in the component functions $y_0, y_1, \ldots$.

The Adomian polynomials are defined through the generating formula [21, 17]

$$A_n = \frac{1}{n!}\frac{d^n}{d\lambda^n}\left[\mathcal{N}\left(\sum_{k=0}^{n} \lambda^k y_k\right)\right]_{\lambda=0}, \tag{2.5}$$

which is valid for analytic nonlinearities. In practice only the first few A_n are required, and they can be tabulated or computed using symbolic algebra.

Remark 2.1. For polynomial nonlinearities $\mathcal{N}(y)$ the first Adomian polynomials can be written explicitly. For example, if $\mathcal{N}(y) = y^2$ then

$$A_0 = y_0^2, \qquad A_1 = 2y_0y_1, \qquad A_2 = 2y_0y_2 + y_1^2, \qquad \ldots$$

These expressions are reminiscent of the binomial expansion and make ADM attractive for nonlinear problems where Taylor expansions become cumbersome.

2.2. **Recursive scheme.** Substituting (2.3) and (2.4) into (2.2), the components are determined by the recurrence

$$y_0(t) = y_0 + J_t[g], \tag{2.6}$$

$$y_{n+1}(t) = J_t[\mathcal{A}y_n + A_n], \qquad n \geq 0. \tag{2.7}$$

The first term y_0 incorporates the initial condition and the forcing, while higher components successively correct the approximation by feeding back the nonlinear contributions through

the integrals. In many applications the series (2.3) converges rapidly, so that a truncated sum

$$\phi_N(t) = \sum_{n=0}^{N-1} y_n(t)$$

already provides an accurate approximation on a finite time interval.

For a *linear* problem

$$\frac{dy}{dt} + \alpha y = g(t), \qquad y(0) = y_0, \tag{2.8}$$

with $\mathcal{N} \equiv 0$, the recurrence simplifies to

$$y_0 = y(0) + \int_0^t g(s)\, ds, \qquad y_{n+1} = -\alpha \int_0^t y_n(s)\, ds, \quad n \geq 0. \tag{2.9}$$

In this case each component is obtained by a single quadrature of the previous one. The sequence of integrals appearing in (2.9) resembles Picard iteration, but the ADM representation often converges faster because the integrals are evaluated only once, and higher-order information is built into the analytic expressions for y_n.

Remark 2.2. The convergence of ADM for general nonlinear problems has been studied in a number of works [8, 12, 1]. Under suitable Lipschitz and boundedness assumptions on f, the series $\sum_{n\geq 0} y_n(t)$ converges uniformly on compact time intervals, and the sum solves the original IVP (2.1). In this paper we do not revisit these general convergence results, but instead focus on how the truncated series behaves in the stiff regime.

2.3. **Example: scalar test equation.** For the Dahlquist test equation

$$y' = \lambda y, \qquad y(0) = 1,$$

we have $\mathcal{A}y = \lambda y$, $\mathcal{N} \equiv 0$ and $g(t) \equiv 0$. From (2.7) we obtain $y_0(t) = 1$ and

$$y_{n+1}(t) = -(-\lambda) \int_0^t y_n(s)\, ds = \lambda \int_0^t y_n(s)\, ds.$$

A simple induction shows that $y_n(t) = (\lambda t)^n / n!$, so that

$$\phi_N(t) = \sum_{n=0}^{N-1} \frac{(\lambda t)^n}{n!}, \tag{2.10}$$

which is the $(N-1)$-th partial sum of $e^{\lambda t}$. Setting $z = \lambda h$ for a single step of size h, the *stability function* of the N-term truncated ADM is therefore

$$R_N(z) = \sum_{n=0}^{N-1} \frac{z^n}{n!}. \tag{2.11}$$

The closed absolute stability region is $\mathcal{S}_N = \{z \in \mathbb{C} : |R_N(z)| \leq 1\}$. This is a bounded subset of $\mathbb{C}$ for every finite N, and it never covers the entire left half-plane, so truncated ADM is *not* A-stable [11, 6]. This observation is the starting point of our stability analysis in Section 4.

Remark 2.3. Even though the exact amplification e^z is stable throughout the left half-plane, the truncated series (2.11) behaves like the stability function of an explicit one-step method and has a bounded absolute-stability region. Increasing N extends its useful range, particularly on the negative real axis, but no finite N recovers the full left half-plane. This limitation motivates the multistage and Laplace-based modifications developed next.

3. Modified ADM Schemes

The limitations of classical ADM for stiff problems have led to several variants designed to enlarge the effective stability region or accelerate convergence without sacrificing the semi-analytical character of the method. In this section we describe two such modifications in detail: Multistage ADM (MADM) and the Laplace–Adomian Decomposition Method (LADM). We also briefly comment on source-splitting variants.

3.1. Multistage ADM (MADM).

Let $0 = t_0 < t_1 < \cdots < t_M = T$ be a mesh with $h_j = t_{j+1} - t_j$ and $h = \max_j h_j$. MADM applies a fresh N-term decomposition on every interval $I_j = [t_j, t_{j+1}]$ and restarts it from the preceding numerical endpoint [15, 9]. Write $Y_0 = y_0$ and introduce the local coordinate $\tau = t - t_j \in [0, h_j]$. The local components and restart are

$$y_0^{[j]}(\tau) = Y_j + \int_0^\tau g(t_j + s)\, ds, \tag{3.1}$$

$$y_{n+1}^{[j]}(\tau) = \int_0^\tau \left[\mathcal{A} y_n^{[j]}(s) + A_n^{[j]}(s)\right] ds, \quad n = 0, \ldots, N-2, \tag{3.2}$$

$$\Phi_j(\tau) = \sum_{n=0}^{N-1} y_n^{[j]}(\tau), \qquad Y_{j+1} = \Phi_j(h_j). \tag{3.3}$$

Here $A_n^{[j]}$ is formed from the local components $y_0^{[j]}, \ldots, y_n^{[j]}$. The number of retained terms is fixed at N on every subinterval. The experiments use the uniform choice $h_j = h = T/M$.

For the Dahlquist equation, subinterval j maps Y_j to $R_N(\lambda h_j) Y_j$. Hence

$$Y_M = \prod_{j=0}^{M-1} R_N(\lambda h_j) y_0. \tag{3.4}$$

Stability requires $\lambda h_j \in \mathcal{S}_N^{\mathrm{ADM}}$ on every subinterval. For a negative real eigenvalue λ, the uniform-step condition is $h \le \beta_N / |\lambda|$, where $[-\beta_N, 0]$ is the negative-real stability interval derived in Section 4.

Remark 3.1. From the numerical point of view, MADM is a restarted explicit one-step construction of order $N - 1$ under the hypotheses of Theorem 5.2. Its step-size constraint is governed by the truncated ADM stability region. Each subinterval also produces a local semi-analytical expression that can be evaluated before the next restart.

3.2. Laplace–Adomian Decomposition Method (LADM).

LADM applies the Laplace transform $\mathcal{L}$ to the ODE before decomposing [13]. For the general equation $y' + \alpha y = \mathcal{N}(y) + g(t)$:

$$s\,\mathcal{L}\{y\} - y_0 + \alpha\,\mathcal{L}\{y\} = \mathcal{L}\{\mathcal{N}(y)\} + \mathcal{L}\{g\}, \tag{3.5}$$

so

$$\mathcal{L}\{y\} = \frac{y_0}{s+\alpha} + \frac{1}{s+\alpha}\left[\mathcal{L}\{\mathcal{N}(y)\} + \mathcal{L}\{g\}\right]. \tag{3.6}$$

The series $y = \sum y_n$ and the Adomian expansion $\mathcal{N}(y) = \sum A_n$ are substituted, and the recurrence becomes

$$\mathcal{L}\{y_0\} = \frac{y_0}{s+\alpha} + \frac{\mathcal{L}\{g\}}{s+\alpha}, \tag{3.7}$$

$$\mathcal{L}\{y_{n+1}\} = \frac{1}{s+\alpha}\,\mathcal{L}\{A_n\}, \qquad n \geq 0. \tag{3.8}$$

Time-domain components are recovered via $y_n(t) = \mathcal{L}^{-1}\{\mathcal{L}\{y_n\}\}$. The key advantage is that the selected stiff linear term αy is represented by the resolvent factor $(s+\alpha)^{-1}$ rather than expanded as a polynomial in αt [13, 22].

The choice of transformed operator is part of the definition of an LADM implementation. More generally, for

$$\mathbf{y}' = B\mathbf{y} + \mathbf{F}(t, \mathbf{y}),$$

we place the specified constant matrix B in the transformed linear operator and obtain

$$\widehat{\mathbf{y}}(s) = (sI - B)^{-1}\mathbf{y}_0 + (sI - B)^{-1}\mathcal{L}\{\mathbf{F}(t, \mathbf{y})\}.$$

If the problem is linear, $\mathbf{y}' = A\mathbf{y} + \mathbf{g}(t)$, and the complete matrix A is chosen as B, exact inversion of the forcing transform places the exact solution in the zeroth component. The homogeneous case is formalised in Theorem 5.3. If $\mathbf{F}$ contains a nonlinearity or a residual linear term $(A-B)\mathbf{y}$, higher Adomian components are nonzero and a finite LADM truncation is generally not exact.

For the scalar test equation $y' = \lambda y$ (i.e. $\alpha = -\lambda$, $\mathcal{N} \equiv 0$, $g \equiv 0$), LADM gives $\mathcal{L}\{y_0\} = 1/(s-\lambda)$, so $y_0(t) = e^{\lambda t}$—the exact solution in a single term.

Remark 3.2. If only part B of a stiff linear operator A is absorbed, the resolvent treats the modes represented by B exactly, while $(A - B)\mathbf{y}$ remains in the decomposition recurrence. Robustness may improve when B captures the dominant stiff modes, but exactness and A- or L-stability do not follow for a finite truncation. They must be analysed for the chosen splitting.

3.3. **Other source-splitting ADM approaches.** Besides MADM and LADM, a number of authors have proposed modified decomposition schemes which adjust the splitting $f = \mathcal{A}y + \mathcal{N}(y) + g$ or add correction terms to accelerate convergence [20, 14, 5]. Typical strategies include:

- choosing $\mathcal{A}$ so that the homogeneous part captures a useful portion of the right-hand-side operator;
- introducing auxiliary parameters to control the size of the Adomian polynomial contributions;
- combining ADM with collocation or Runge–Kutta ideas to obtain hybrid schemes.

While these techniques can be effective on a case-by-case basis, they usually do not change the underlying stability function for stiff linear test problems. In contrast, MADM and LADM have a clear and analysable impact on stability, which is why we focus on them in the sequel.

4. Stability Analysis

We analyse absolute stability for the Dahlquist test equation $y' = \lambda y$ by comparing each method's stability function $R(z)$, where $z = \lambda h$. This section derives the truncated ADM and MADM stability functions and contrasts their regions with classical A- and L-stable implicit Runge–Kutta schemes. The goal is to quantify how the multistage strategy enlarges the effective stability domain for stiff problems.

4.1. **Stability function of truncated ADM.** Let Y_j approximate $y(t_j)$ and set $\tau = t - t_j$. For $y' = \lambda y$, the local ADM recurrence is

$$y_0^{[j]}(\tau) = Y_j, \qquad y_{n+1}^{[j]}(\tau) = \lambda \int_0^\tau y_n^{[j]}(s)\, ds.$$

Induction gives $y_n^{[j]}(\tau) = Y_j(\lambda\tau)^n/n!$. Therefore an N-term step of length h satisfies

$$Y_{j+1} = \sum_{n=0}^{N-1} y_n^{[j]}(h) = \left(\sum_{n=0}^{N-1} \frac{(\lambda h)^n}{n!}\right) Y_j = R_N(z) Y_j, \qquad z = \lambda h.$$

This establishes, rather than assumes, the amplification factor in (2.11). We use the standard closed absolute-stability region

$$\mathcal{S}_N^{\mathrm{ADM}} = \{z \in \mathbb{C} : |R_N(z)| \le 1\}; \tag{4.1}$$

its interior is obtained by replacing $\le$ with $<$. The boundary is the algebraic curve $|R_N(x + \mathrm{i}y)| = 1$.

The complex regions need not be nested pointwise as N changes. Nevertheless, $R_N \to e^z$ uniformly on compact sets, so every compact subset of the open left half-plane is contained in $\mathcal{S}_N^{\mathrm{ADM}}$ for all sufficiently large N. For every finite N, however, the region remains bounded. On the negative real axis its connected component containing the origin is $[-\beta_N, 0]$. The corrected values in Table 1 show its growth with the truncation length.

Table 1. Real stability boundary β_N for N-term truncated ADM: $|R_N(-\beta_N)| = 1$.

N (terms)	Stability function	β_N (approx.)
2	$1 + z$	2.0000
3	$1 + z + z^2/2$	2.0000
4	$1 + z + z^2/2 + z^3/6$	2.5127
5	$\sum_{k=0}^{4} z^k/k!$	2.7853
6	$\sum_{k=0}^{5} z^k/k!$	3.2170

For the autonomous scalar test equation the implicit midpoint and trapezoidal rules have the same stability function, $R(z) = (2 + z)/(2 - z)$, and are A-stable. The two-stage Radau IIA method has

$$R_{\mathrm{Radau}}(z) = \frac{1 + z/3}{1 - 2z/3 + z^2/6};$$

it is third order and L-stable [11, 7].

4.2. **Stability function of MADM.** MADM with M equal subintervals inside a macro-interval of length H uses the local step $\delta = H/M$. With the macro-parameter $z = \lambda H$, applying the local factor successively gives

$$R_N^{(M)}(z) = \big[R_N(z/M)\big]^M. \tag{4.2}$$

Consequently,

$$\begin{aligned} \mathcal{S}_{N,M}^{\mathrm{MADM}} &= \{z : |R_N(z/M)|^M \le 1\} \\ &= \{z : z/M \in \mathcal{S}_N^{\mathrm{ADM}}\} = M\mathcal{S}_N^{\mathrm{ADM}}. \end{aligned} \tag{4.3}$$

Thus the MADM macro-stability region is exactly the dilation by M of the single-subinterval ADM region; its negative-real interval is $[-M\beta_N, 0]$. It is bounded, and hence not A-stable, for every finite M and N. For each fixed z with $\operatorname{Re} z < 0$, however, z/M eventually lies in $\mathcal{S}_N^{\mathrm{ADM}}$ as M grows. Moreover, for $N \ge 2$,

$$\log R_N(z/M) = z/M + O(M^{-2}), \qquad [R_N(z/M)]^M \longrightarrow e^z.$$

These statements quantify both the stability enlargement and the limiting exact amplification.

TABLE 2. Comparison of stability properties of ADM-based and implicit Runge–Kutta methods.

Method	Order	A-stable?	L-stable?	Stability function	Work per step
ADM (N terms)	$N-1$	No	No	$R_N(z)$	$N-1$ recursions
MADM (N terms)	$N-1$	No	No	$R_N(z)$ per subinterval	$N-1$ recursions
LADM (linear)	Exact	Yes†	Yes†	e^z	one linear transform solve
Implicit midpoint	2	Yes	No	$(2+z)/(2-z)$	one implicit stage
Trapezoidal rule	2	Yes	No	$(2+z)/(2-z)$	one nonlinear solve
Radau IIA ($s=2$)	3	Yes	Yes	$\dfrac{1+z/3}{1-2z/3+z^2/6}$	two coupled stages

†Exact only when the complete constant linear operator is absorbed.

4.3. **Comparison with implicit Runge–Kutta methods.** Truncated ADM and every finite-subinterval MADM construction have bounded regions, whereas the three IRK methods cover the closed left half-plane. Radau IIA additionally damps infinitely stiff modes because $R(z) \to 0$ as $z \to -\infty$; midpoint and trapezoidal satisfy $R(z) \to -1$ and therefore are not L-stable. LADM removes the polynomial stability restriction only for the linear operator treated exactly. Figure 1 displays these distinctions.

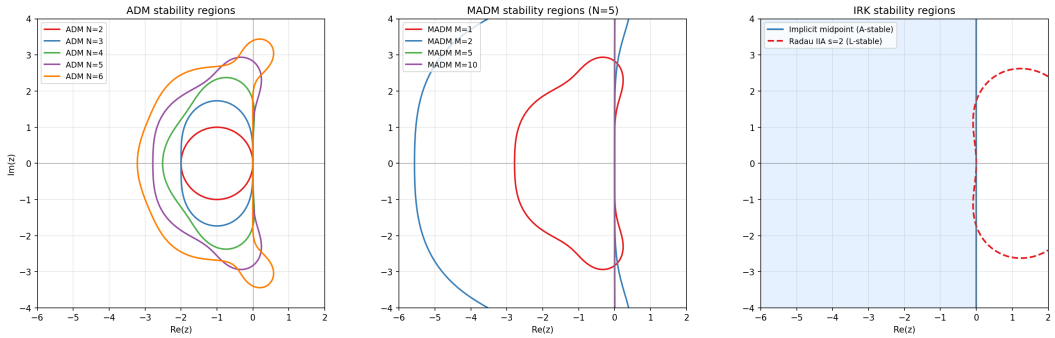

FIGURE 1. Absolute stability regions in the complex z–plane. Left: truncated ADM for $N = 2, \ldots, 6$. Middle: MADM with $N = 5$ and different numbers of subintervals M. Right: A-stable implicit midpoint rule and L-stable two-stage Radau IIA method.

5. Convergence and Stability Theorems

We now formalise the stability and convergence properties that underlie the numerical comparisons. The first result characterises the truncated ADM stability function and its bounded absolute stability region. The second establishes global convergence of MADM for Lipschitz initial value problems.

Theorem 5.1 (Stability characterisation of truncated ADM)**.** *Consider the test equation $y' = \lambda y$, $y(0) = 1$, and the N-term truncated ADM applied with step size h. Let $z = \lambda h$ and define the stability function*

$$R_N(z) = \sum_{k=0}^{N-1} \frac{z^k}{k!}.$$

Then:

(a) $R_N(z)$ is the $(N-1)$-th Taylor polynomial of e^z at the origin, and therefore $R_N(z) \to e^z$ uniformly on compact subsets of $\mathbb{C}$ as $N \to \infty$.

(b) For every finite $N \geq 2$, the absolute stability region $\mathcal{S}_N = \{z \in \mathbb{C} : |R_N(z)| \leq 1\}$ is bounded. Consequently, truncated ADM is not A-stable.

(c) Define

$$\beta_N = \sup\{b > 0 : |R_N(-x)| \leq 1 \text{ for every } x \in [0, b]\}.$$

Then $0 < \beta_N < \infty$ and the negative-real component of $\mathcal{S}_N$ containing the origin is exactly $[-\beta_N, 0]$. Its endpoint satisfies $R_N(-\beta_N) = -1$ for even N and $R_N(-\beta_N) = 1$ for odd N.

Proof. **Part (a).** By definition, $R_N(z) = \sum_{k=0}^{N-1} z^k/k!$ is the $(N-1)$-th partial sum of the Maclaurin series of e^z. Since the exponential series converges absolutely and uniformly on any compact set $K \subset \mathbb{C}$, we have $\sup_{z \in K} |R_N(z) - e^z| \leq \sum_{k=N}^{\infty} |z|^k/k! \to 0$ as $N \to \infty$.

Part (b). The function $R_N(z)$ is a polynomial of degree $N-1$. For $|z|$ large, $|R_N(z)| \sim |z|^{N-1}/(N-1)! \to \infty$. Therefore $|R_N(z)| > 1$ for $|z|$ sufficiently large, which means $\mathcal{S}_N$

is bounded. Since A-stability requires $\mathcal{S} \supseteq \mathbb{C}^-$, which is unbounded, the truncated ADM cannot be A-stable.

Part (c). Since $R_N(0) = 1$ and $R_N(-x) = 1 - x + O(x^2)$, one has $|R_N(-x)| < 1$ for all sufficiently small $x > 0$. Part (b) implies that the connected stable interval cannot extend to infinity, so $0 < \beta_N < \infty$ and continuity gives $|R_N(-\beta_N)| = 1$. The leading term of $R_N(-x)$ has sign $(-1)^{N-1}$; hence the first exit is through -1 when N is even and through $+1$ when N is odd. The numerical endpoints in Table 1 are obtained from these scalar equations. □

Theorem 5.2 (Convergence of MADM for smooth Lipschitz IVPs)**.** *Let $f : [0, T] \times \mathbb{R}^d \to \mathbb{R}^d$ be locally Lipschitz in y and suppose that the IVP* (2.1) *has a unique solution whose graph lies in a compact set K. Fix $N \geq 2$ and assume that f is C^N on a neighbourhood of K, with all derivatives through order N bounded there. Assume also that the standard local ADM decomposition is well defined and retains the terms through degree $N - 1$. Then there are constants $h_0, C > 0$, independent of the mesh, such that for every mesh with $h = \max_j h_j \leq h_0$,*

$$\max_{0 \leq j \leq M} \|y(t_j) - Y_j\| \leq C \, \frac{e^{LT} - 1}{L} \, h^{N-1}, \tag{5.1}$$

where L is a Lipschitz constant on that neighbourhood and $(e^{LT} - 1)/L$ is interpreted as T when $L = 0$. Thus fixed-N MADM has global order $N - 1$.

Proof. The smoothness assumptions and the standard Adomian construction imply that the local truncated series agrees with the exact time expansion through degree $N - 1$. Taylor's theorem therefore gives a uniform local defect

$$\|\varphi_{h_j}(y(t_j)) - \Phi_j(h_j; y(t_j))\| \leq C_{\mathrm{loc}} h_j^N,$$

where φ_h is the exact flow and Φ_j is the N-term local ADM map. On the same compact neighbourhood, the numerical map is locally Lipschitz:

$$\|\Phi_j(h_j; u) - \Phi_j(h_j; v)\| \leq (1 + L h_j + C_0 h_j^2) \|u - v\|.$$

For sufficiently small h the quadratic term can be absorbed into a mesh-independent constant $\widetilde{L}$. With $e_j = y(t_j) - Y_j$,

$$\|e_{j+1}\| \leq (1 + \widetilde{L} h_j) \|e_j\| + C_{\mathrm{loc}} h_j^N.$$

The discrete Gronwall inequality [11], $e_0 = 0$, and $\sum_j h_j = T$ yield

$$\max_j \|e_j\| \leq C_{\mathrm{loc}} e^{\widetilde{L} T} \sum_{j=0}^{M-1} h_j^N \leq C_{\mathrm{loc}} T e^{\widetilde{L} T} h^{N-1},$$

which has the stated form after changing the constant. □

Theorem 5.3 (LADM exactness for linear constant-coefficient systems)**.** *Consider the linear system $\mathbf{y}' = A\mathbf{y}$, $\mathbf{y}(0) = \mathbf{y}_0$, where $A \in \mathbb{R}^{n \times n}$ is constant, the solution is of exponential order, and the complete matrix A is included in the transformed linear operator. Then LADM produces the exact solution $\mathbf{y}(t) = e^{At}\mathbf{y}_0$ in the zeroth component alone; all higher components vanish.*

Proof. Applying the Laplace transform to $\mathbf{y}' = A\mathbf{y}$ gives $s\hat{\mathbf{y}}(s) - \mathbf{y}_0 = A\hat{\mathbf{y}}(s)$, so $\hat{\mathbf{y}}(s) = (sI - A)^{-1}\mathbf{y}_0$. In the LADM recurrence (3.7)–(3.8) with α replaced by $-A$, $g \equiv 0$ and $\mathcal{N} \equiv 0$:

$$\mathcal{L}\{\mathbf{y}_0\} = (sI - A)^{-1}\mathbf{y}_0, \qquad \mathcal{L}\{\mathbf{y}_{n+1}\} = \frac{1}{sI - A}\,\mathcal{L}\{A_n\} = \mathbf{0} \quad \text{for all } n \geq 0,$$

since all Adomian polynomials vanish. Inverting gives $\mathbf{y}_0(t) = e^{At}\mathbf{y}_0$ and $\mathbf{y}_n(t) = \mathbf{0}$ for $n \geq 1$. □

6. Test Problems, Exact Solutions and Numerical Results

For each test problem, a closed-form exact solution or a high-accuracy reference solution is used to compare classical ADM, MADM, LADM where applicable, implicit midpoint, trapezoidal and two-stage Radau IIA. The following definitions and protocol are used throughout.

For a scalar component q, with errors $e_j = q_{\mathrm{ref}}(t_j) - q_j$ on the common mesh, define

$$E_\infty(q) = \max_{0 \leq j \leq M} |e_j|, \qquad E_2(q) = \left[\sum_{j=0}^{M-1} \frac{h_j}{2}\left(|e_j|^2 + |e_{j+1}|^2\right)\right]^{1/2}. \tag{6.1}$$

All methods are evaluated at the same mesh nodes, so neither norm benefits from interpolation on a finer output grid. The label *Divergent* is used only when the computed solution grows by orders of magnitude relative to the bounded reference; otherwise a finite error is reported.

All computations use IEEE double precision. Unless stated otherwise, ADM and MADM retain $N = 5$ components, i.e. terms through degree four. The local coefficients were generated from the Adomian recurrence; equivalently for these analytic ODEs, they were evaluated by repeated total differentiation of $y' = f(t, y)$. The three IRK methods use the identical uniform step $h = T/M$. Their nonlinear algebraic equations are initialized with an explicit-Euler predictor and iterated until the residual infinity norm is below 10^{-12}. Work is reported as four coefficient evaluations per MADM step and as the measured number of right-hand-side calls for IRK methods. CPU values are medians of five runs on one AMD EPYC 9V74 processor using Python 3.13, NumPy 2.4 and SciPy 1.17; they are implementation-dependent and are included only as a reproducibility indicator. The fixed-step formulas, solver tolerances, reference-solution settings and output grids needed to reproduce the reported comparisons are specified in this section.

Problem 1: Stiff scalar decay. Consider the scalar IVP with large stiffness parameter λ:

$$\frac{dy}{dt} = \lambda\,(y - \cos t) - \sin t, \qquad y(0) = 1, \qquad \lambda = -50. \tag{6.2}$$

Rewriting: $y' - \lambda y = -\lambda\cos t - \sin t$. The integrating factor is $e^{-\lambda t}$, and we obtain

$$y(t)e^{-\lambda t} = 1 + \int_0^t e^{-\lambda s}\big(-\lambda\cos s - \sin s\big)\,ds.$$

Evaluating the integral using the standard formula $\int e^{as}\cos(bs)\,ds = \frac{e^{as}(a\cos bs + b\sin bs)}{a^2+b^2}$ and simplifying, the exact solution reduces to

$$y_{\mathrm{exact}}(t) = \cos t. \tag{6.3}$$

This can be verified by direct substitution. The stiffness arises because a perturbation from $\cos t$ is damped at rate e^{-50t}, creating a thin initial layer when the starting value is perturbed.

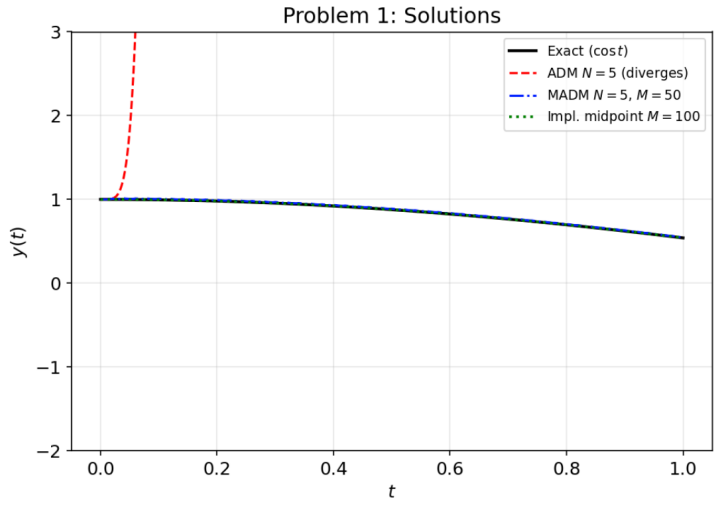

FIGURE 2. Problem 1: solutions for the stiff decay problem with $\lambda = -50$. The exact solution is compared with the truncated ADM ($N = 5$), the multistage ADM (MADM, $N = 5$ and $M = 50$) and the implicit midpoint rule with $M = 100$ steps.

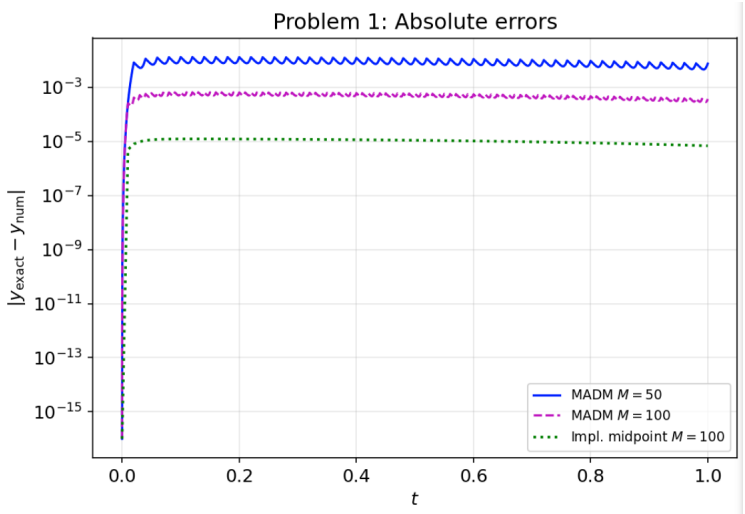

FIGURE 3. Problem 1: absolute errors $|y_{\text{exact}} - y_{\text{num}}|$ for MADM with $M = 50$ and $M = 100$ subintervals and for the implicit midpoint rule with $M = 100$ steps.

Classical ADM ($N = 5$, one interval). For the unperturbed initial value, cancellations reduce the global degree-four approximation to $1 - t^2/2 + t^4/24$, so it does not blow up on $[0, 1]$ and has $E_\infty = 1.36 \times 10^{-3}$. This special cancellation does not remove the stability defect: a perturbation satisfies the homogeneous amplification polynomial $R_5(-50t)$ and is strongly amplified outside the stability interval.

MADM ($N = 5$). With $M = 100$ and $h = 0.01$, the local parameter is $z = -0.5$, which lies well inside $[-\beta_5, 0] = [-2.7853, 0]$. Table 3 shows fourth-order convergence until roundoff begins to dominate.

LADM. Taking the Laplace transform of (6.2) with $\alpha = -\lambda = 50$ absorbs the complete linear operator. Exact inversion of the forcing transform yields $y_0(t) = \cos t$, so no higher component is needed for this problem.

TABLE 3. Errors for Problem 1 ($\lambda = -50$, $T = 1$), using the norms in (6.1).

Method	Terms/order	Subintervals/steps	E_∞	E_2
ADM	$N = 5$	1	1.36×10^{-3}	3.80×10^{-4}
MADM	$N = 5$	$M = 50$	3.52×10^{-11}	2.14×10^{-11}
MADM	$N = 5$	$M = 100$	1.76×10^{-12}	1.07×10^{-12}
MADM	$N = 5$	$M = 200$	9.77×10^{-14}	5.97×10^{-14}
LADM	exact linear solve	1	$< 10^{-15}$	$< 10^{-15}$
Implicit midpoint	order 2	$M = 100$	1.24×10^{-5}	1.05×10^{-5}

At the matched step size $h = 0.01$, MADM is more accurate than the second-order midpoint rule, while LADM is exact because it absorbs the complete linear operator. Table 6 also reports trapezoidal and Radau IIA results at this same step size.

Problem 2: Stiff linear 2×2 system. Consider the system [18]

$$\frac{d}{dt}\begin{pmatrix} y_1 \\ y_2 \end{pmatrix} = \begin{pmatrix} -100 & 1 \\ 0 & -1 \end{pmatrix}\begin{pmatrix} y_1 \\ y_2 \end{pmatrix}, \qquad \begin{pmatrix} y_1(0) \\ y_2(0) \end{pmatrix} = \begin{pmatrix} 1 \\ 1 \end{pmatrix}. \tag{6.4}$$

The eigenvalues of A are $\lambda_1 = -100$ and $\lambda_2 = -1$ (stiffness ratio $= 100$). The matrix A is upper triangular, so the system decouples:

$$y_2(t) = e^{-t}, \tag{6.5}$$

$$y_1' = -100\, y_1 + e^{-t}, \qquad y_1(0) = 1. \tag{6.6}$$

Solving (6.6) with integrating factor e^{100t}:

$$y_1(t)e^{100t} = 1 + \int_0^t e^{99s}\, ds = 1 + \frac{1}{99}(e^{99t} - 1).$$

Hence the exact solution is

$$y_{1,\mathrm{exact}}(t) = \frac{98}{99}\, e^{-100t} + \frac{1}{99}\, e^{-t}, \qquad y_{2,\mathrm{exact}}(t) = e^{-t}. \tag{6.7}$$

The component y_1 has a rapidly decaying transient $\frac{98}{99}e^{-100t}$ and a slowly decaying mode $\frac{1}{99}e^{-t}$. A degree-four ADM polynomial on the entire interval cannot represent the fast

exponential and reaches magnitude 3.96×10^6. With $M = 100$, however, $z_1 = -1$ lies safely in $[-2.7853, 0]$, and MADM resolves both modes.

TABLE 4. Errors for Problem 2 ($T = 1$), using the common-grid norms in (6.1).

Method	Subintervals/steps	$E_\infty(y_1)$	$E_2(y_1)$	$E_\infty(y_2)$	$E_2(y_2)$
ADM ($N = 5$)	1	3.96×10^{6}	1.32×10^{6}	7.12×10^{-3}	2.18×10^{-3}
MADM ($N = 5$)	50	1.96×10^{-1}	3.10×10^{-2}	4.99×10^{-10}	3.85×10^{-10}
MADM ($N = 5$)	100	7.05×10^{-3}	9.39×10^{-4}	3.09×10^{-11}	2.39×10^{-11}
LADM (complete A)	1	$< 10^{-15}$	$< 10^{-15}$	$< 10^{-15}$	$< 10^{-15}$
Impl. midpoint	100	3.42×10^{-2}	4.41×10^{-3}	3.07×10^{-6}	2.37×10^{-6}

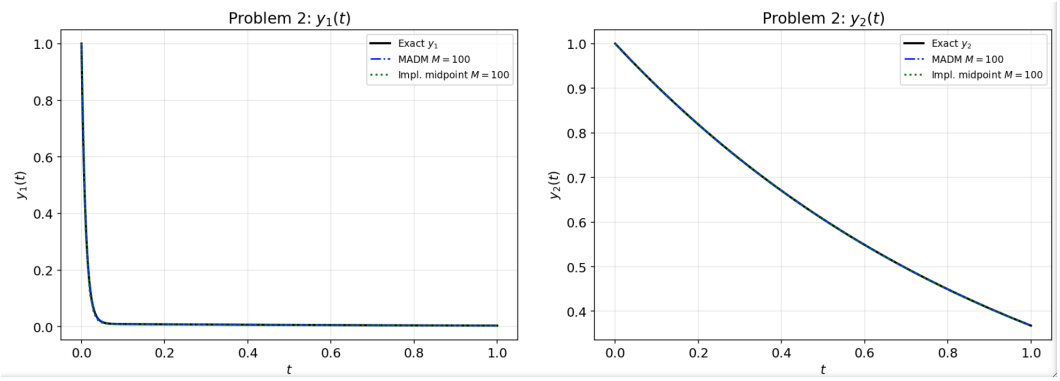

FIGURE 4. Problem 2: solutions for the stiff 2×2 system. The exact solution components $y_1(t)$ and $y_2(t)$ are compared with the MADM approximation ($N = 5$, $M = 100$) and the implicit midpoint rule with $M = 100$ steps.

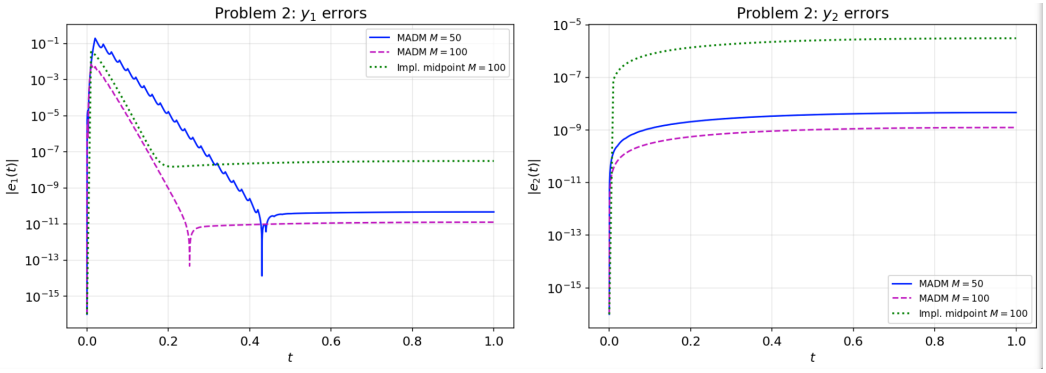

FIGURE 5. Problem 2: absolute errors for y_1 and y_2 under MADM with $M = 50$ and $M = 100$ subintervals, and the implicit midpoint rule with $M = 100$ steps.

For the slow component, $|z_2| = 0.02$ at $M = 50$, and MADM is already close to roundoff. For the fast component, $z_1 = -2$ at $M = 50$ is stable but yields appreciable truncation error; halving the step moves it to $z_1 = -1$ and reduces $E_\infty(y_1)$ to 7.05×10^{-3}. At the common value $M = 100$, MADM is more accurate than midpoint and trapezoidal but less accurate than two-stage Radau IIA for y_1; see Table 6.

Problem 3: Van der Pol oscillator (stiff regime). The Van der Pol oscillator with large parameter μ is a classical stiff nonlinear test problem [11]:

$$y_1' = y_2, \qquad y_2' = \mu\,(1 - y_1^2)\,y_2 - y_1, \qquad y_1(0) = 2, \quad y_2(0) = 0. \tag{6.8}$$

For $\mu = 20$, the system is moderately stiff. No closed-form solution exists. The reference was computed with SciPy's variable-step fifth-order Radau implementation using rtol $= 10^{-13}$, atol $= 10^{-14}$ and dense output. The run used 1758 accepted steps, 12332 right-hand-side evaluations, 4 Jacobian evaluations and 76 LU factorizations. Repeating the computation at the smallest relative tolerance allowed by the implementation changed the comparison-grid values by less than 4×10^{-14}.

The nonlinearity $N(y_1, y_2) = \mu(1 - y_1^2)y_2$ generates Adomian polynomials [21, 17]:

$$\begin{aligned} A_0 &= \mu(1 - y_{1,0}^2)y_{2,0}, \\ A_1 &= \mu\big[(1 - y_{1,0}^2)y_{2,1} - 2y_{1,0}y_{1,1}y_{2,0}\big], \\ A_2 &= \mu\big[(1 - y_{1,0}^2)y_{2,2} - 2y_{1,0}y_{1,2}y_{2,0} - 2y_{1,0}y_{1,1}y_{2,1} - (y_{1,1}^2)y_{2,0}\big]. \end{aligned}$$

The trajectory drifts along attracting slow branches and undergoes rapid transitions. A single degree-four ADM polynomial grows to magnitudes above 10^5 on $[0, 5]$, whereas MADM with $M = 500$, $h = 0.01$ tracks both slow and fast portions accurately. Increasing to $M = 1000$ gives the fourth-order decrease shown in Table 5.

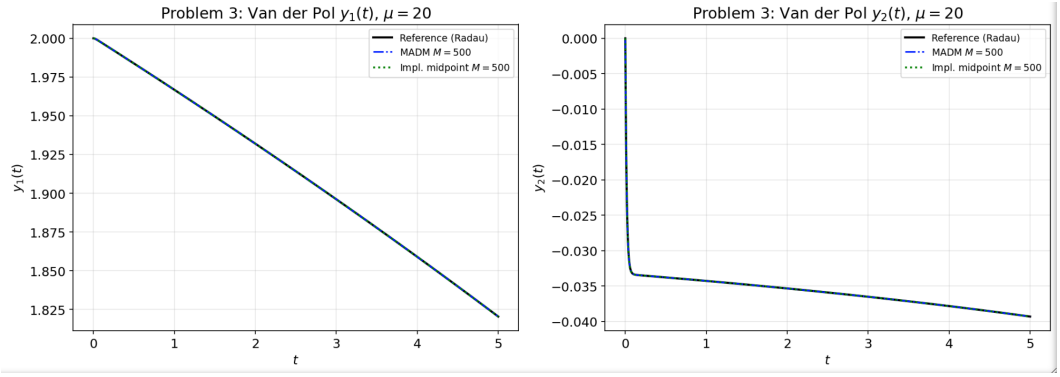

FIGURE 6. Problem 3: Van der Pol oscillator with $\mu = 20$. Reference solution (Radau) compared with MADM ($N = 5$, $M = 500$) and the implicit midpoint rule with $M = 500$ steps.

At $M = 500$, the MADM errors are about 17 times smaller than the midpoint errors in each component. Its accuracy is also comparable to fixed-step two-stage Radau IIA, while requiring no nonlinear stage solve. This is an accuracy comparison at a matched step size,

not a claim of identical computational cost; the measured work and timings are separated in Table 6.

TABLE 5. Errors for Problem 3 relative to the high-accuracy Radau reference.

Method	Subintervals/steps	$E_\infty(y_1)$	$E_2(y_1)$	$E_\infty(y_2)$	$E_2(y_2)$
ADM ($N = 5$)	1	Divergent	Divergent	Divergent	Divergent
MADM ($N = 5$)	200	2.79×10^{-5}	5.02×10^{-6}	1.66×10^{-3}	2.99×10^{-4}
MADM ($N = 5$)	500	3.60×10^{-7}	6.43×10^{-8}	2.14×10^{-5}	3.81×10^{-6}
MADM ($N = 5$)	1000	1.77×10^{-8}	3.14×10^{-9}	1.05×10^{-6}	1.86×10^{-7}
Impl. midpoint	500	6.25×10^{-6}	1.11×10^{-6}	3.75×10^{-4}	6.64×10^{-5}

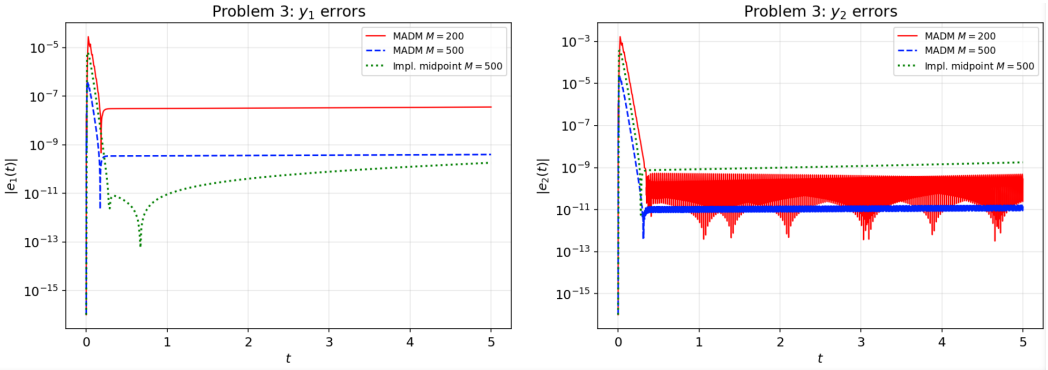

FIGURE 7. Problem 3: absolute errors in y_1 and y_2 for MADM with $M = 200$ and $M = 500$ subintervals, and for the implicit midpoint rule with $M = 500$ steps, relative to the Radau reference solution.

6.1. **Overall comparison.** Table 6 gives the requested controlled comparison. The step counts are $M = 100$ for Problems 1–2 and $M = 500$ for Problem 3, so every row within a problem uses the same h. The error columns use the definitions in (6.1); vector entries are ordered as (y_1, y_2). Work and time are reported separately because one symbolic coefficient evaluation is not equivalent to one nonlinear IRK stage evaluation.

TABLE 6. Matched-step accuracy, measured work and CPU time. Vector errors are ordered as (y_1, y_2). *Coeff.* denotes a local ADM coefficient evaluation and *RHS* a right-hand-side evaluation made during the implicit solves; these work units are reported separately and are not assumed to have equal cost.

Problem (h)	Method	E_∞	E_2	Work	CPU (ms)
P1 (10^{-2})	MADM, $N=5$	1.76×10^{-12}	1.07×10^{-12}	400 coeff.	1.5
	midpoint	1.24×10^{-5}	1.05×10^{-5}	1106 RHS	4.3
	trapezoidal	1.38×10^{-7}	8.48×10^{-8}	710 RHS	3.3
	Radau IIA (2)	1.42×10^{-8}	8.76×10^{-9}	2766 RHS	22.2
P2 (10^{-2})	MADM, $N=5$	$(7.05\times10^{-3}, 3.09\times10^{-11})$	$(9.39\times10^{-4}, 2.39\times10^{-11})$	400 coeff.	1.2
	midpoint	$(3.42\times10^{-2}, 3.07\times10^{-6})$	$(4.41\times10^{-3}, 2.37\times10^{-6})$	1274 RHS	5.2
	trapezoidal	$(3.42\times10^{-2}, 3.07\times10^{-6})$	$(4.41\times10^{-3}, 2.37\times10^{-6})$	866 RHS	3.2
	Radau IIA (2)	$(4.20\times10^{-3}, 5.10\times10^{-9})$	$(5.55\times10^{-4}, 3.94\times10^{-9})$	3070 RHS	22.8
P3 (10^{-2})	MADM, $N=5$	$(3.60\times10^{-7}, 2.14\times10^{-5})$	$(6.43\times10^{-8}, 3.81\times10^{-6})$	2000 coeff.	11.1
	midpoint	$(6.25\times10^{-6}, 3.75\times10^{-4})$	$(1.11\times10^{-6}, 6.64\times10^{-5})$	5603 RHS	21.8
	trapezoidal	$(6.25\times10^{-6}, 3.75\times10^{-4})$	$(1.11\times10^{-6}, 6.64\times10^{-5})$	6581 RHS	23.5
	Radau IIA (2)	$(5.28\times10^{-7}, 3.17\times10^{-5})$	$(9.39\times10^{-8}, 5.63\times10^{-6})$	14858 RHS	102.2

Table 6 does not identify one method as uniformly best. For Problem 1, MADM has the smallest error among the fixed-step methods. For Problem 2, Radau IIA gives the smaller fast-component error, $E_\infty(y_1) = 4.20\times10^{-3}$ versus 7.05×10^{-3} for MADM, whereas MADM gives the smaller slow-component error and the lower measured runtime. For Problem 3, MADM's errors are slightly smaller than the fixed-step Radau IIA errors in both components, but the two methods have the same broad accuracy scale. Midpoint and trapezoidal are less accurate on these particular meshes, while their A-stability remains valuable outside the MADM stability restriction. Thus observed accuracy must be read together with component, step size, work model and stability properties. LADM is exact for the two linear problems when the complete linear operator is transformed, but that analytic preprocessing is qualitatively different from a fixed-step solve and is therefore not assigned a CPU ranking.

7. CONCLUSION

Three Adomian-based strategies—classical truncated ADM, MADM and LADM—were formulated and analysed for stiff IVPs. The N-term stability function is the degree-$(N-1)$ Taylor polynomial $R_N(z) = \sum_{k=0}^{N-1} z^k/k!$, so its stability region is bounded. For M equal MADM subintervals, the macro-stability region is exactly $M\mathcal{S}_N$, not an A-stable region for finite M. Under explicit smoothness, bounded-derivative and Lipschitz hypotheses, fixed-N MADM has global order $N-1$. LADM recovers the exact linear solution only when the complete constant linear operator is transformed and the remaining transforms are inverted exactly; partial absorption leaves a nonzero truncated recurrence.

The revised experiments use common meshes, common error norms, stated nonlinear tolerances, work counts and CPU timings. At $h = 0.01$, five-component MADM gives smaller errors than midpoint and trapezoidal for the reported tests. Relative to two-stage

Radau IIA, the outcome is component-dependent: Radau is more accurate for the fast component of Problem 2, whereas MADM is more accurate for its slow component and is slightly more accurate in both components of Problem 3. MADM also has the lower measured runtime in this implementation, although its coefficient evaluations and the IRK right-hand-side evaluations are not identical units of work. Classical one-interval ADM is inaccurate or unstable except when special cancellation occurs, and LADM is exact only when the complete linear problem is absorbed and inverted exactly. These results support MADM as a useful semi-analytical option when its explicit stability restriction is satisfied; they do not replace the unconditional stability advantages of established IRK solvers.

References

[1] K. Abbaoui and Y. Cherruault, Convergence of Adomian's method applied to differential equations, Comput. Math. Appl., 28 (1994), no. 5, 103–109.

[2] G. A. Adomian, A review of the decomposition method in applied mathematics, J. Math. Anal. Appl., 135 (1988), no. 2, 501–544.

[3] G. A. Adomian, *Solving frontier problems of physics: the decomposition method*, Fundamental Theories of Physics, 60, Kluwer Acad. Publ., Dordrecht, 1994.

[4] G. A. Adomian and R. C. Rach, Modified Adomian polynomials, Math. Comput. Modelling, 24 (1996), no. 11, 39–46.

[5] E. Babolian and J. Biazar, Solution of nonlinear equations by modified Adomian decomposition method, Appl. Math. Comput., 132 (2002), no. 1, 167–172.

[6] J. Biazar, E. Babolian and M. R. Islam, Solution of a system of Volterra integral equations of the first kind by Adomian method, Appl. Math. Comput., 139 (2003), no. 2-3, 249–258.

[7] J. C. Butcher, *Numerical methods for ordinary differential equations*, third edition, Wiley, Chichester, 2016.

[8] Y. Cherruault, Convergence of Adomian's method, Kybernetes, 18 (1989), no. 2, 31–38.

[9] S. M. El-Sayed and D. Kaya, On the numerical solution of the system of two-dimensional Burgers' equations by the decomposition method, Appl. Math. Comput., 158 (2004), no. 1, 101–109.

[10] M. A. Fabio, S. A. Seminara and M. I. Troparevsky, Approximate solutions to fractional boundary value problems by wavelet decomposition methods, in *Applications of wavelet multiresolution analysis*, 1–21, SEMA SIMAI Springer Ser., 4, Springer, Cham.

[11] E. Hairer and G. Wanner, *Solving ordinary differential equations. II*, second edition, Springer Series in Computational Mathematics, 14, Springer, Berlin, 1996.

[12] M. M. Hosseini and H. Nasabzadeh, On the convergence of Adomian decomposition method, Appl. Math. Comput., 182 (2006), no. 1, 536–543.

[13] S. A. Khuri, A Laplace decomposition algorithm applied to a class of nonlinear differential equations, J. Appl. Math., 1 (2001), no. 4, 141–155.

[14] X.-G. Luo, A two-step Adomian decomposition method, Appl. Math. Comput., 170 (2005), no. 1, 570–583.

[15] N. Ngarasta, J. Rodoumta and H. Kankou, Solving nonlinear stiff differential equations using multistage Adomian decomposition method, International Journal of Pure and Applied Mathematics, 55 (2009), 563–578.

[16] A. Orellana Castillo, S. A. Seminara and M. I. Troparevsky, Regular pairs for solving Fredholm integral equations of the second kind, Poincare J. Anal. Appl., 2018, no. 2, 47–56.

[17] R. C. Rach, A new definition of the Adomian polynomials, Kybernetes, 37 (2008), no. 7, 910–955.

[18] S. Sekar and A. Kavitha, Numerical solution of the linear and nonlinear stiff problems using Adomian decomposition method, IOSR Journal of Mathematics, 11 (2015), 14–20.

[19] S. A. Seminara and M. I. Troparevsky, Convergence of Adomian decomposition method for PDEs, Poincare J. Anal. Appl., 2016, no. 1, 1–12.
[20] A.-M. Wazwaz, A reliable modification of Adomian decomposition method, Appl. Math. Comput., 102 (1999), no. 1, 77–86.
[21] A.-M. Wazwaz, A new algorithm for calculating Adomian polynomials for nonlinear operators, Appl. Math. Comput., 111 (2000), no. 1, 53–69.
[22] A.-M. Wazwaz and M. S. Mehanna, The combined Laplace-Adomian method for handling singular integral equation of heat transfer, Int. J. Nonlinear Sci., 10 (2010), no. 2, 248–252.
[23] D. G. Yakubu and A. M. Kwami, Lobatto–Runge–Kutta collocation and Adomian decomposition methods on stiff differential equations, International Journal of Mathematics and Computation, 28 (2017), 1–13.

©Poincare Publishers, India